THE AMERICAN SOCIETY OF MECHANICAL ENGINEERS
345 E. 47th St., New York, N.Y. 10017

98-GT-92

DETAILED MEASUREMENTS WITHIN A SELECTION OF PIPE DIFFUSERS FOR CENTRIFUGAL COMPRESSORS

I. Bennett, A. Tourlidakis and R.L. Elder
Cranfield University
Cranfield, Bedfordshire, England

ABSTRACT

It is well established that the flow between the impeller tip and the diffuser throat is very influential on the performance and flow range of a centrifugal compressor stage. Detailed measurements of a parametric selection of pipe diffusers have been carried out within this region using a combination of conventional pneumatic and high speed pressure transducers.

Four pipe diffuser designs were examined. The first and datum consisted of 31 pipes, representing a design with minimal meridional step (or sidewall expansion) between impeller tip and diffuser throat. The step size was increased to 1.3 for the second design resulting in a 22 pipe diffuser. A further increase of sidewall expansion ratio to 1.7 with 13 pipes was completed following favourable results from the 22 pipe tests. The final diffuser was of hybrid design consisting of an oval rather than circular throat cross-section. This departure allowed for a 13 pipe diffuser without sidewall expansion.

Flow range and performance comparisons are made in addition to detailed measurements which clearly show that strong planar pulsations dominate the distorted diffuser throat flow. Larger pressure pulsations are quantified for the designs with low numbers of pipes.

NOMENCLATURE

$C_{p,i\text{-}j}$ static pressure recovery coefficient $= \left(\frac{p_j - p_i}{p_{oi} - p_i}\right)$

D diameter
m mass flow
M Mach number
P pressure
PR pressure ratio (total-total)
R radius
W passage width
β impeller backsweep (from radial)
ω impeller rotational speed

Subscripts
le diffuser leading edge
d design condition
ps pressure surface
pvs pseudo-vaneless space
ss suction surface
th diffuser throat
o total or stagnation conditions

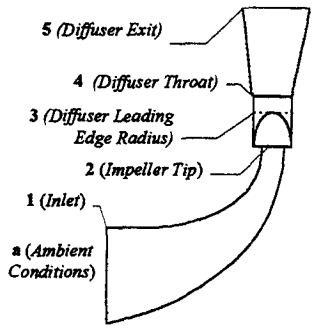

Fig. 1 Measurement Plane Designations

INTRODUCTION

The geometry of the region between the impeller tip and diffuser throat is accepted as being very influential, little understood and crucial to the performance of centrifugal compressors. Pipe diffusers are described in the literature (e.g. Kenny (1969, 1970, 1972) and Reeves (1977)) as potentially being an improvement over conventional vane island diffusers. Based on

Presented at the International Gas Turbine & Aeroengine Congress & Exhibition
Stockholm, Sweden — June 2–June 5, 1998

these claims, improvements in compressor efficiency have been thought possible with the use of pipe diffusers, particularly at higher pressure ratios.

As introduced, probably the most complex flow region in a centrifugal compressor is that between the impeller tip and diffuser throat where an unsteady distorted impeller flow interacts with the complex geometry of the diffuser inlet. Diffusers are particularly little understood in this area and the objective of this current research has been to shed some light on this complex region.

This paper describes a series of experiments to define the flow within the leading edge region of four pipe diffusers and a vaneless diffuser. The vaneless experiments were undertaken to define the flow discharging from the impeller into the diffuser.

TEST RIG AND INSTRUMENTATION

Impeller details are shown in Fig. 2 and Table 1.

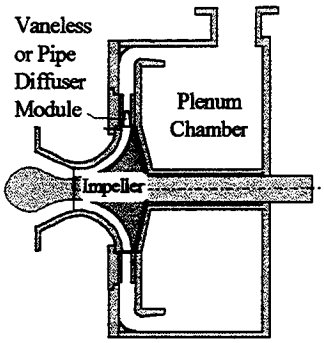

Table 1 Impeller Details

Pressure Ratio	5.3
Speed (rpm)	34,825
Corr. Design Mass Flow (kg/sec)	4.1
Blades	17
Tip Diameter, D_2 (m)	0.29253
W_2 (m)	0.01175
Backsweep, β (deg)	24°
Rake	8°
Tip Clearance (mm)	0.3

Fig. 2 Description of Compressor

In the vaneless configuration, the flow discharged at a tip speed of 533 m/s into a parallel walled diffuser which extended up to 1.50 times the impeller tip radius (see Fig. 2). This was followed by an abrupt step from 12.05mm to 21.54mm width at entry into another parallel section. The flow was then turned, at an impeller tip radius ratio of 2.19, by a bend of constant normal flow area. Finally, the flow was diffused by an annular diffuser of area ratio 2 prior to dumping into a large plenum. The abrupt step and relatively wide discharge width were incorporated to allow pipe diffuser modular sections to be easily inserted.

The four diffusers examined are shown in Fig. 3. and details are given in Table 2. It should be noted that in this study the conical portion of the diffusers were not modelled and the flow was abruptly dumped after the diffuser throat into the wide vaneless diffuser seen in Fig. 2. It is considered that this influenced surge, but the flow in upstream components was believed largely representative. This simplification reduced individual build costs and was necessary to allow a wide range of diffusers to be examined. In all cases the cylindrical 'throat' portions were set equal to 1 hydraulic diameter long.

The first and datum diffuser (Design A) consisted of 31 pipes, representing the traditional design with minimal step (or sidewall expansion). Sidewall expansion is a phenomenon particular to pipe diffusers formed from cylindrical drillings and may be expressed as the relationship between the diameter of the pipe drillings and the number of pipes (see Fig. 4). Such an expansion is necessitated by the fixed total throat area. The second diffuser (Design B), allowed a reduction in the number of pipes down to 22 by incorporating a sidewall expansion ratio of 1.3. A further increase in expansion ratio to 1.7 with 13 pipes (Design C) was completed following favourable experimental results from the previous designs. The increment from 1.3 to 1.7 is somewhat larger than would have been desirable and was undertaken in order to avoid having the same number of pipes as impeller blades.

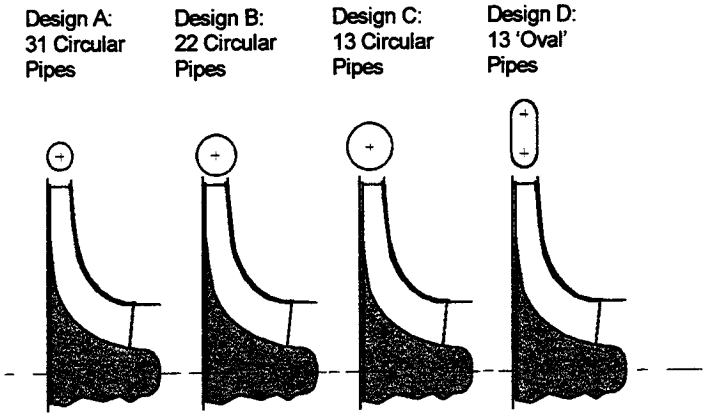

Fig. 3 Sketch of Tested Pipe Diffuser Configurations

Table 2 Details of Tested Pipe Diffusers

Pipe Diffuser	No. of Pipes	Sidewall Expansion W_3/W_2	Leading Edge, D_3/D_2	Throat Area (mm^2)	Range Improvement (%)*
A	31	1.105	1.101	4290	-
B	22	1.311	1.078	4290	15%
C	13	1.707	1.071	4290	32%
D	13	1.05	1.071	4290	32%

* Percentage of 31 pipe diffuser flow range (choke to surge)

In order to assess the effect of a large sidewall expansion step, a 13 pipe diffuser with an oval throat cross section was designed, following the work of Reeves, 1977 (Design D). This design incorporated minimal sidewall expansion, thus fixing the radii required for throat construction. Working with a fixed throat area then allowed the prescription of the distance between the centres of the two construction radii. The oval pipe diffuser was designed with the same leading edge radius as the 13 circular pipe diffuser. This meant using a pipe drilling tangency radius other than the impeller tip as used for the other designs. Nominally, for all 4 pipe diffusers, choking occurred at 103.8% of the design mass flow (the impeller inducer choked at 105.6%).

The motivation to examine diffusers with smaller numbers of pipes was driven by the desire to increase stage operating range. Previous work by Elder and Gill (1984) and Rodgers and Sapiro (1972) for vane island diffusers, and Groh et al (1969) and Japikse (1980) for pipe diffusers, had shown that significant range enhancements were possible. The range increases found in this present investigation are shown in Table 2, displaying improvements of up to 32% for the 13 pipe designs. These improvements, however, should be viewed with caution as the downstream diffusing cone was omitted.

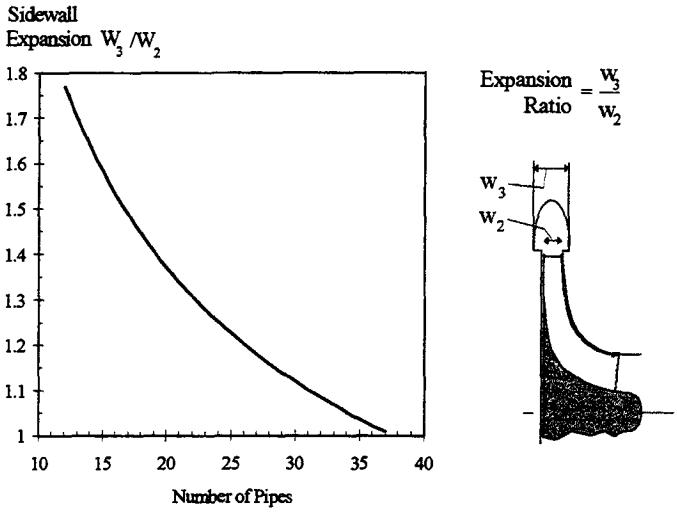

Fig. 4 Effect of Number of Pipes on Sidewall Expansion Ratio

Detailed traverses were carried out using ultra-miniature fast response pressure transducers. These were individually mounted and could be axially traversed and rotated about an axis perpendicular to their sensor faces (see Fig. 5). Probe movement was achieved using an electromechanical traverse mechanism purposely built for the current investigation (see Bennett (1997)).

Fig. 5 Pressure Transducer Mounting

At each measurement location, the flow angle and total pressure were determined by curve fitting a series of 7 measurements taken at steps of 10°. The sensor arrangement was sufficiently small such that it did not excessively influence the very small domain of interest. The curve fitting of angular measurements to get flow angle and total pressure was carried out using a cosine curve fit and single value decomposition (Press et al, 1989).

The pressure transducers used (Kulite XCE-062) were shown sensitive to temperature and it was necessary to include additional compensation to correct for these variations. The method used was similar to that outlined by Cherrett (1990) and required the calibration of pressure and temperature against transducer supply current and output potential. In addition, these traverses were repeated with a pneumatic total pressure probe substituted for the transducer to confirm the unsteady instrumentation measurements.

Table 3 shows the experimental uncertainties of both measurement systems. Note that the transducer total pressure error for *amplitude* is approximately only ± 0.02 Bar. The large *absolute* error shown in Table 3 is due to drift.

Table 3 Experimental Errors

Pressure Probe Type	Pressure Error	Angular Error
Pneumatic	± 0.005 Bar	–
Transducer	± 0.2 Bar	± 3°

FLOW MEASUREMENTS AT THE IMPELLER TIP

The mounted fast response pressure transducers shown in Fig. 5 were used to traverse the impeller tip in order to gain an appreciation of the flow entering the diffuser. Traverses were carried out whilst in the vaneless configuration and it was possible to map both total pressure and flow angle. The high spatial measurement resolution is shown below in Fig. 6. In the circumferential direction, for the full speed investigations, readings were taken at 333kHz, giving 34 measurement locations per blade passage. Each location was ensemble averaged 500 times (measurements were triggered once per revolution).

At design flow (and incidentally all the other measured flow conditions not shown here), there are two distinct peaks of high total pressure (see Fig. 7). The highest of these is located near the blade suction surface and the other, joined by a small saddle, presents itself almost mid-channel. Of particular interest is the blade suction surface peak where a region of low pressure is expected due to blade separation. Examination of the relative total pressure provides the more familiar wake picture typical for centrifugal compressor flows, showing a region of poor flow (relative to the impeller passage) near the suction/shroud corner. In addition, a region of low relative total pressure and near tangential flow (90° flow angle) is seen virtually along the complete shroud surface. The combination of these factors indicates a large region of shroud separated flow. Integrated values of mass weighted total pressure and flow angle agreed with the overall rig instrumentation to within 2.7% in total pressure and 2.3° in flow angle.

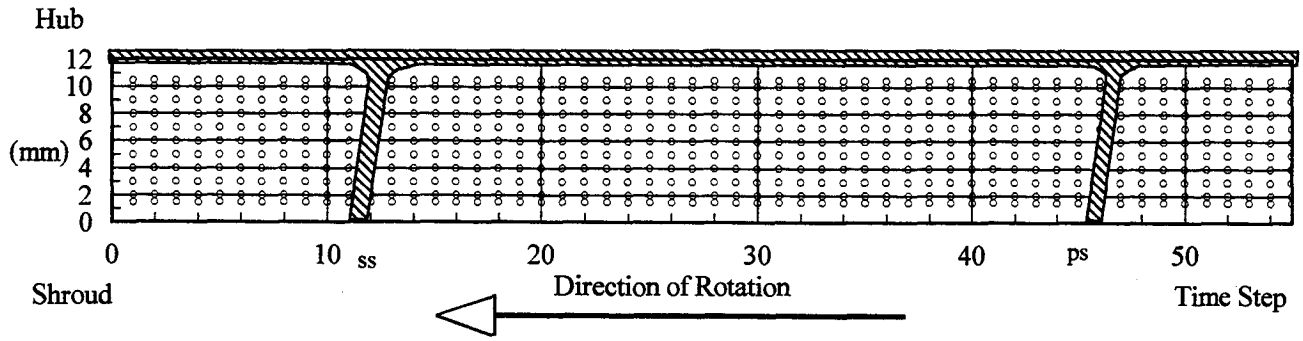

Fig. 6 Sketch Showing the High Spatial Resolution of Traverse and Approximate Blade Location

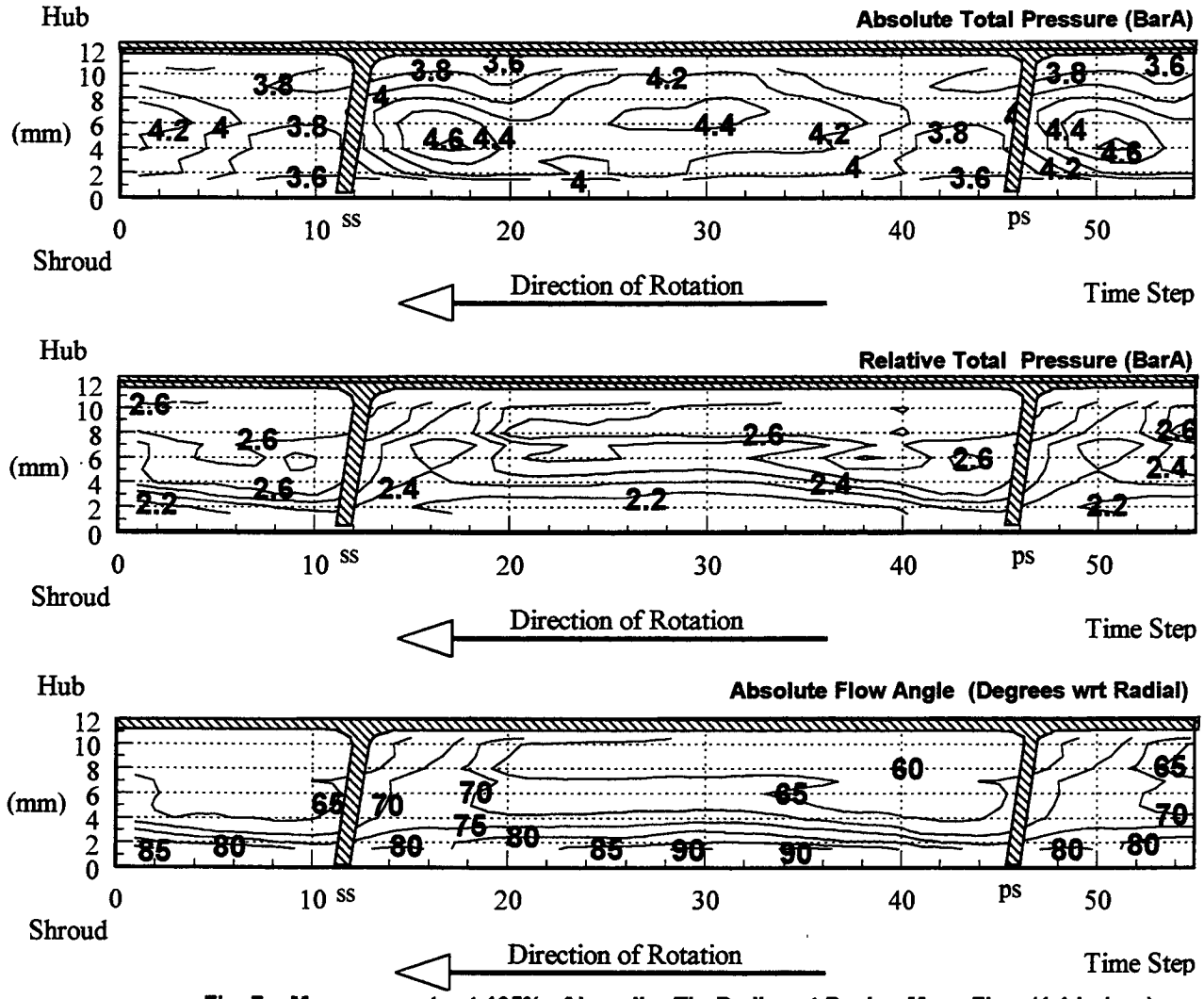

Fig. 7 Measurements at 105% of Impeller Tip Radius at Design Mass Flow (4.1 kg/sec)

FLOW WITHIN THE VANELESS, PSEUDO- AND SEMI-VANELESS SPACES OF PIPE DIFFUSERS

The flow exiting the impeller of the test centrifugal compressor has been shown to include regions of high and low total pressure that in the stationary frame result in a highly-unsteady incident flow to the downstream diffuser. The diffuser inlet region must accept this flow and convert velocity head into useful static pressure by the most efficient means possible. There is generally strong diffusion in this region which may result in excessive total pressure losses together with the possibility of introducing flow with large blockage into the downstream diffuser channel. The latter is important as it has been well documented that diffuser channel effectiveness drops severely when the throat blockage is large (e.g. Dolan and Runstadler (1973)).

The pseudo-vaneless space includes partially spanning vanes that grow to bridge the passage width as the throat is approached (see Fig. 8). Midway between them, radial diffusion is expected in a manner akin to that seen in a vaneless diffuser. Near these vanes, however, the flow is locally influenced. The resulting flow structure in this region therefore contains strong 3D flows.

Figure 9 displays the Mach number distribution within the vaneless, pseudo- and semi- vaneless spaces of the 13 (oval-section) pipe diffuser. At all flow conditions, the Mach number was calculated using the impeller tip total pressure[+] and no account is made for losses. The most distinctive feature that differentiated the pipe diffusers tested with low numbers of pipes was the near-continual (apart possibly near choke) presence of a leading edge shock suggested by these measurements. Similar deductions were made by Japikse (1980) in an earlier study of pipe diffusers. For the diffuser with 13 (oval) pipes, a pseudo-vaneless space acceleration is seen from the nominal (vaneless) impeller tip value of M=1.05 and this occurs at all flow rates. Then, just prior to the leading edge wedge, there is a rapid deceleration of the flow. This is characteristic of a shock and is particularly pronounced at lower mass flows.

[+] Impeller tip total pressure was calculated using the measured impeller tip static pressure, 5% impeller tip blockage and the conservation of energy.

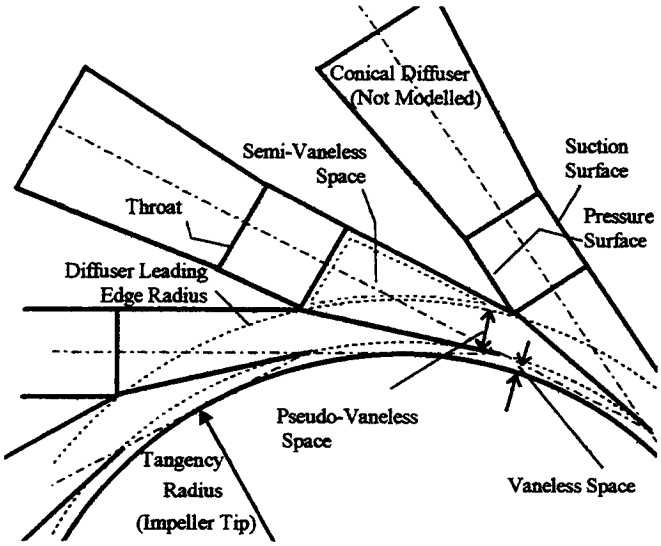

Fig. 8 Sketch of a Pipe Diffuser

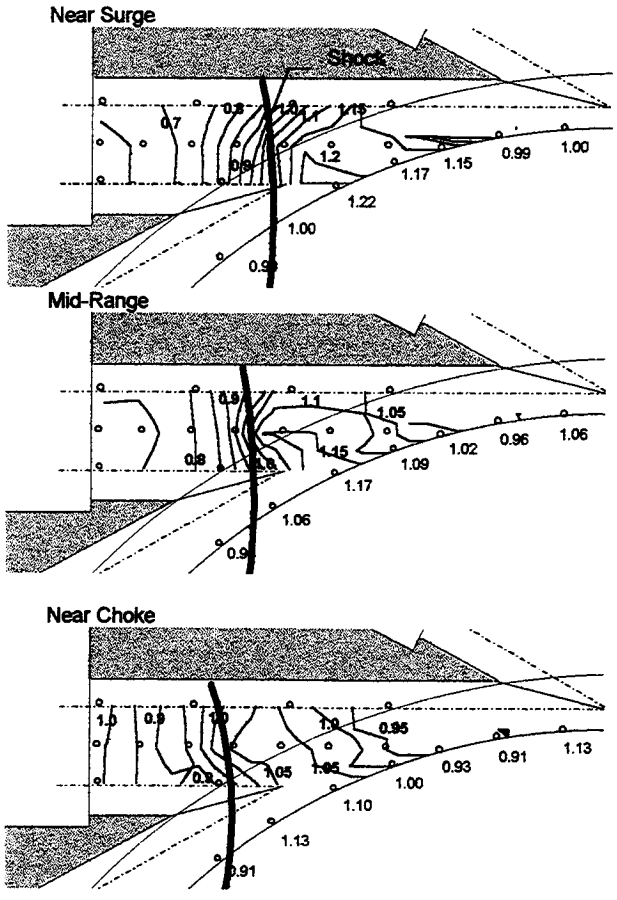

Fig. 9 Mach Number Distribution within Pseudo- and Semi- Vaneless Spaces of 13 (Oval) Pipe Diffuser

THE DIFFUSER THROAT

The diffuser throat is of primary interest to compressor aerodynamicists as the flow in this region has a controlling influence over the downstream cone effectiveness (e.g. Dolan and Runstadler (1973)). The throat flows measured in this investigation show distortion and unsteadiness. Such asymmetries are well known to significantly influence the channel effectiveness (e.g. Japikse and Baines (1984)) and it is for this reason that the diffuser throat flows are thoroughly investigated here.

Throat total pressure measurements of the four diffusers are shown in Fig. 10 (see Fig. 8 for the definition of suction surface, ss, and pressure surface, ps). These measurements were taken using a pneumatic (slow response) equivalent of the total pressure probe shown in Fig. 5 with a 0.9mm diameter face. Some minor corrections were necessary as the probe required manual relocation for each shroud-to-hub traverse. The overall impeller total pressure ratio was used to scale the 'raw' measurements.

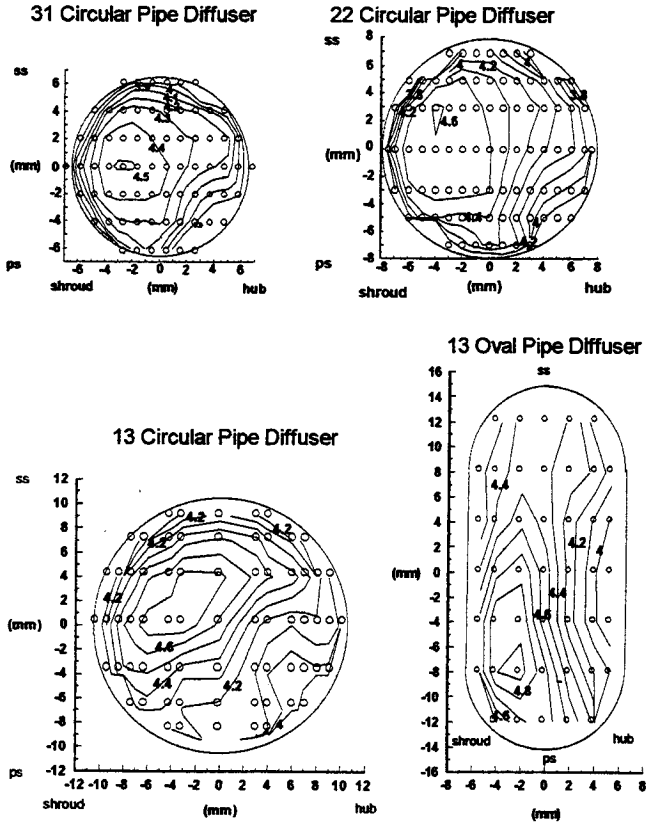

Fig. 10 Total Pressure at Diffuser Throats (BarA)

For each circular diffuser there is one distinct total pressure peak located near the shroud with, diametrically opposite, a low pressure region. The shape and location of the total pressure fields did not vary with mass flow. Interestingly, the position of the total pressure peak for the oval configuration is, whilst still close to the shroud, much closer to the pressure surface than for the other configurations. The oval configuration also provides some evidence of the lower pressure region but in this case it spans much of the hub-side surface. In an attempt to understand the flow mechanism, an examination of incidence did not yield any consistent correlation.

FLOW DISTORTION BETWEEN THE IMPELLER TIP AND DIFFUSER THROAT

During testing, the major disadvantage noted of the configurations with fewer pipes was the noticeable increase in flow distortion within the vaneless, pseudo-vaneless and semi- vaneless spaces. These are of concern to designers as excessively high unsteady aerodynamic loadings can be transmitted to rotating components leading to high cycle fatigue even at normal operating conditions.

Circumferential distortions in static pressure at the impeller tip are caused by the downstream influence of the diffuser. Such distortions were measured using a series of circumferentially placed static pressure tappings at the impeller exit. The effect of each pipe diffuser design on the impeller tip static pressure distortion over each respective operational range, is shown in Fig. 11. The vaneless diffuser values were included to give some idea of the accuracy of static pressure measurements at the impeller tip because there should theoretically be no distortion in the vaneless configuration.

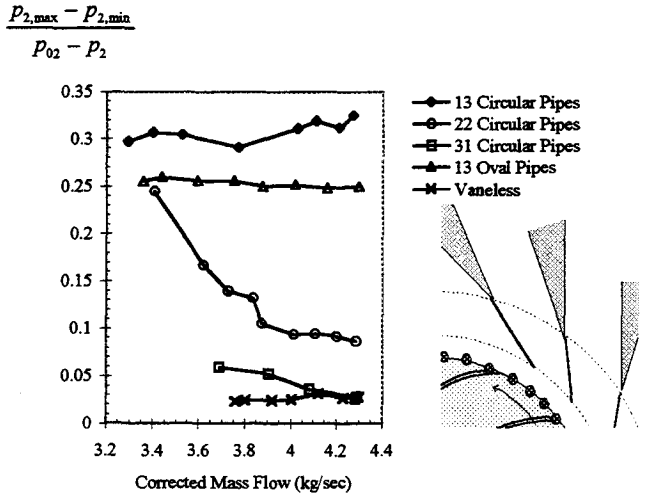

Fig. 11 Impeller Tip Static Pressure Distortion

Static pressure distortions at impeller tip may be regarded as a measure of the flow unsteadiness imposed on the rotating frame. The large differences between diffuser configurations are expected to be caused by many effects including incidence, pipe diffuser leading edge radius, impeller tip Mach number and diffuser leading edge aerodynamic loading. Analysis of the measured Mach number distributions such as those shown in Fig. 9, indicated that the distortion was significantly influenced by the presence of leading edge shocks which penetrated the impeller periphery. Such shocks were particularly prevalent in configurations with few pipes and this is reflected in their elevated values of distortion in Fig. 11. A similar investigation was also carried out by Japikse (1980) who also showed stronger shock structures for diffusers with lower numbers of pipes. He attributed two impeller failures to peripheral static pressure field distortion.

Flow unsteadiness in the stationary frame was detected using high speed pressure transducers. These were located within the pseudo-vaneless-space at a constant radius, $1.04R_2$. This static pressure unsteadiness is presented in terms of range (i.e. max-min) in Fig. 12. These measurements are ensemble averages of 500 samples to remove non-synchronous data. Although there is no consistent trend with the number of pipes, it is clear that the most severe loadings are for the 13 circular pipe diffuser. Generally the unsteadiness rises towards surge but, in the most severe cases, increases towards choke can also be observed. Some alleviation of unsteadiness is found when switching from a circular to an oval 13 pipe design.

Further unsteady static pressure readings also were taken along the diffuser centreline for the 13 oval pipe diffuser and are shown in Fig. 13. These results indicate that near choke the level of unsteadiness increases as the flow progresses through the pseudo- and semi-vaneless spaces. This increase in unsteadiness follows the trends shown by Abdel-Hamid et al (1987) with the static pressure fluctuation amplified by the diffusion process. As the flow rate is decreased, the pseudo-vaneless space unsteadiness remains almost constant but that in the semi-vaneless-space rises steeply. The unsteadiness in the throat-inlet region also increases steadily after a sharp rise near choke whereas that at the throat-outlet, remains high, but somewhat inconsistent with flow rate.

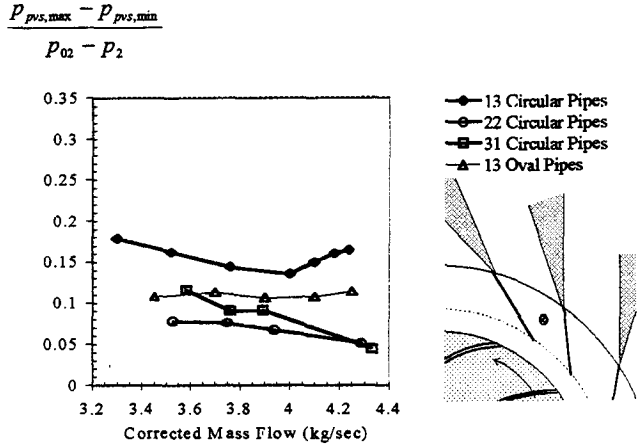

Fig. 12 Static Pressure Unsteadiness within Pseudo-Vaneless-Space

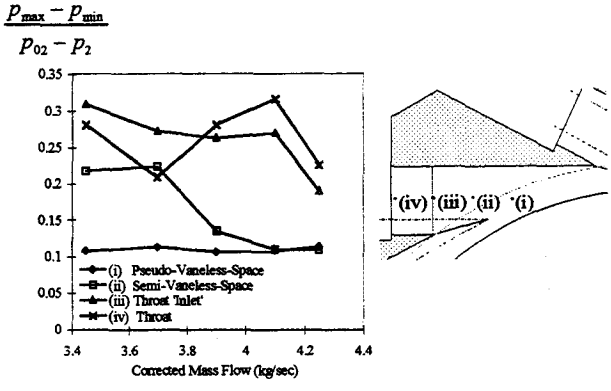

Fig. 13 Static Pressure Unsteadiness within Pseudo- and Semi-Vaneless Spaces

Figure 14 shows the static pressure measurements within the 13 oval pipe diffuser plotted against time. Near choke, the mean levels and amplitude of fluctuation of static pressure are similar. Near surge, however, the mean levels diverge due to diffusion between impeller tip and diffuser throat. As the data acquisition was triggered at the same impeller location in each example, the flow features may be followed through the domain. In particular, two peaks of elevated static pressure per blade pass are seen throughout when operating near-surge (see Fig. 14). It is interesting to note the large magnitude of the diffusion within the pseudo- and semi-vaneless spaces.

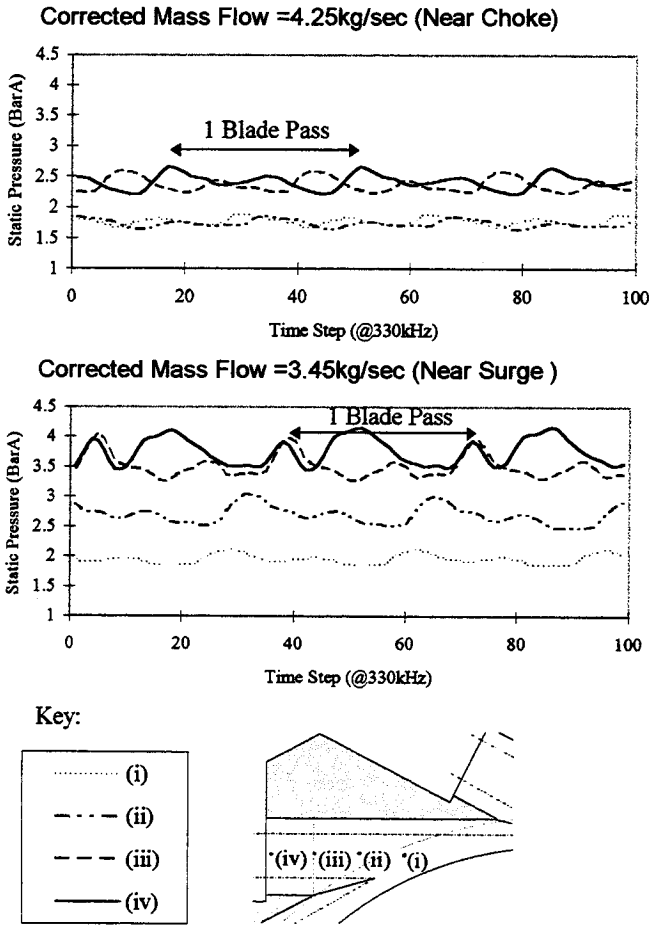

Fig. 14 Static Pressure Measurements within 13 (Oval) Pipe Diffuser Pseudo- and Semi- Vaneless Spaces

Unsteady total pressure measurements were made in the diffuser throat using miniature pressure transducers. Each 'point', defined by both location and time step, was ensemble averaged (triggered once per blade rotation) from 500 samples. For each time step a throat-plane (or planar) average may be calculated. These, when plotted against time, showed a strong total pressure pulsation. Fig. 15 presents the range of throat-plane total pressure amplitudes associated with each of the circular-section pipe diffusers. Stronger pulsations are detected for the pipe diffusers with fewer numbers of pipes.

The planar averages for the 13 (circular) pipe diffuser are plotted against time in Fig. 16. These illustrate the strong pulsations which are a major finding of this work. The amplitude of these pulsations are largely independent of flow rate and show two total pressure peaks per cycle as also measured with the unsteady static pressure instrumentation. Clearly, assuming fully mixed out uniform flow at the diffuser throat, as is often assumed, is grossly incorrect.

Figure 17 shows the throat total pressures at the maxima and minima of the 'design' mass flow trace (points A and B in Fig. 16). These demonstrate how the total pressure field at the throat fluctuated strongly in absolute level but retains surprisingly similar relative planar distributions.

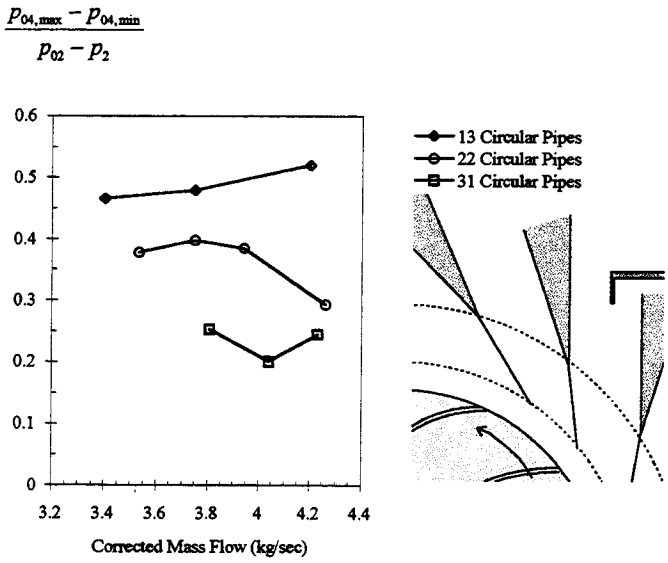

Fig. 15 Planar Total Pressure Unsteadiness at Diffuser Throat

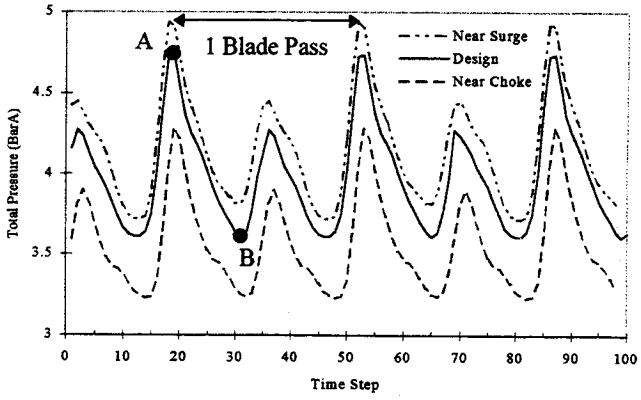

Fig. 16 Planar Total Pressure Pulsations Measured within 13 (Circular) Pipe Diffuser Throat

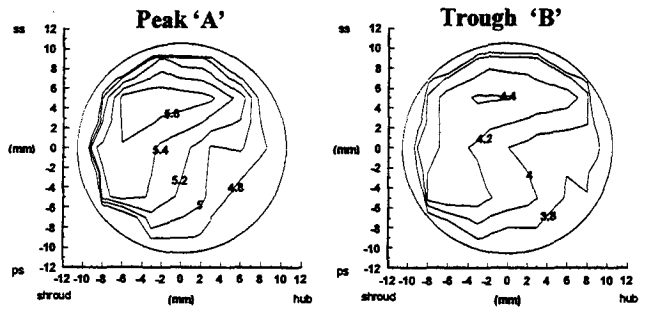

Fig. 17 Instantaneous Total Pressure Distributions within 13 (Circular) Pipe Diffuser Throat

CONCLUSIONS

Detailed measurements have been made within four pipe diffusers using both pneumatic and unsteady total pressure sensors. These have presented the flow between the impeller tip and the diffuser throat as being strongly pulsating, containing large distortions. In particular, the following pertinent conclusions may be drawn from this work:

- Significant range enhancement, as shown in the literature, has been found for pipe diffusers with low numbers of passages. This benefit, however, has been at the cost of increased unsteadiness and flow distortion. Pipe diffusers with lower numbers of pipes are shown to cause significantly larger impeller tip static pressure distortions. These have previously been blamed for impeller failure.
- Unsteady static pressure instrumentation has shown that disturbances are amplified within the pseudo- and semi-vaneless spaces.
- All diffusers have shown a dominating throat total pressure pulsation. Surprisingly, the general form of the throat total pressure field remains largely unchanged in time.
- The largest throat total pressure amplitudes were measured within diffusers with lower numbers of passages. These pulsations clearly arise from the structure of the flow leaving the impeller.

ACKNOWLEDGEMENTS

The research contained within this paper was supported by Engineering and Physical Sciences Research Council, European Gas Turbines and National Power and this is gratefully acknowledged. Thanks must also go to Mr Richard Lutley, for rig construction and assistance in running.

REFERENCES

Abdel-Hamid, A.N., Haupt. U. and Rautenberg, M., 1987, "Unsteady Flow Characteristics in a Centrifugal Compressor with Vaned Diffuser" ASME 87-GT-142, Presented at the International Gas Turbine Conference, Anaheim, California.

Bennett, I., 1997, "The Design and Analysis of Pipe Diffusers for Centrifugal Compressors" Ph.D Thesis, Cranfield University.

Cherrett, M.A., 1990, "Temperature Error Compensation Applied to Pressure Measurements Taken with Miniature Semiconductor Pressure Transducers in a High-Speed Research Compressor" Technical Memo P1192, Royal Aircraft Establishment.

Dolan, X.F. and Runstadler, P.W., 1973, "Pressure Recovery Performance of Conical Diffusers at High Subsonic Mach Numbers" NASA Contractor Report, NASA CR-2299.

Elder, R.L. and Gill, M.E., 1984, "A Discussion of the Factors Affecting Surge in Centrifugal Compressors" ASME 84-GT-194, Presented at the 29th International Gas Turbine Conference, Amsterdam, Netherlands.

Groh, F.G., Wood, G.M., Kulp, R.S. and Kenny, D.P., 1969, "Evaluation of a High Hub/Tip Ratio Centrifugal Compressor" ASME Paper No. 69-WA/FE-28, Journal of Basic Engineering.

Japikse, D., 1980, "The Influence of Diffuser Inlet Pressure Fields on the Range and Durability of Centrifugal Compressor Stages" AGARD Conference Proceedings: "Centrifugal Compressors, Flow Phenomena and Performance" AGARD-CP-282.

Japikse, D. and Baines, N.C., 1994, "Introduction to Turbomachinery" Concepts ETI, Inc., Norwich, Vermont, USA 05055, page 4-24.

Kenny, D.P., 1969, "A Novel Low-Cost Diffuser for High-Performance Centrifugal Compressors" ASME Journal of Engineering for Power, pp37-47.

Kenny, D.P., 1970, "Supersonic Radial Diffusers" AGARD Lecture Series #39, Advanced Compressors, VKI, Brussels, Belgium, June 1-4.

Kenny, D.P., 1972, "A Comparison of the Predicted and Measured Performance of High Pressure Ratio Centrifugal Compressor Duties" VKI Lecture Series No. 50, Advanced Radial Compressors.

Press, W.H. et al., 1989, "Numerical Recipes: the Art of Scientific Computing (FORTRAN version)" Cambridge University Press.

Reeves, G.B., 1977, "Design and Performance of Selected Pipe-Type Diffusers" ASME Paper 77-GT-104.

Rodgers, C. and Sapiro, L., 1972, "Design Considerations for High Pressure Ratio Centrifugal Compressors" ASME 72-GT-91.